Semi-Automated Classification of the Physiological Condition of the Carotid Artery in 2D Ultrasound Image Sequences

HAMED HAMID MUHAMMED [(1)], JIMMY C. AZAR[(2)]

[(1)]Division of Informatics, Logistics and Management
School of Technology and Health (STH)
Royal Institute of Technology (KTH)
Alfred Nobels Alle 10, SE-141 52 Huddinge
SWEDEN

E-mail: hamed.muhammed@sth.kth.se , Tel: +46(0)8-7904855 ,URL: http://www.sth.kth.se/hamed/

[(2)] Centre for Image Analysis
Uppsala University
Box 337, SE-751 05 Uppsala
SWEDEN

E-mail: jimmy.azar@cb.uu.se , Tel: +46(0)18-4713473 , URL: http://www.cb.uu.se/~jimmy/

Abstract: -A novel automated method for the classification of the physiological condition of the carotid artery in 2D ultrasound image sequences is introduced. Unsupervised clustering was applied for the segmentation process in which both spatial and temporal information was utilized. Radial distension is then measured in the inner surface of the vessel wall, and this characteristic signal is extracted to reveal the detailed radial motion of the variable inner part of the vessel wall that is in contact with flowing blood. Characteristic differences in this time signal were noticed among healthy young, healthy elderly and pathological elderly cases. The discrete Fourier transform of the radial distension signal is then computed, and the area subtended by the transform is calculated and utilized as a diagnostic feature. The method was tested successfully and could differentiate among the categories of patients mentioned above. Therefore, this computer-aided method would significantly simplify the task of medical specialists in detecting any defects in the carotid artery and thereby in detecting early cardiovascular symptoms. The significance of the proposed method is that it is intuitive, semi-automatic, reproducible, and significantly reduces the reliance upon subjective measures.

Key-Words: -Unsupervised clustering, ultrasound image segmentation, k-means algorithm, discrete Fourier transform DFT, carotid artery, radial distension.

1 Introduction

According to Gebel [1], 30% of global deaths are caused by cardiovascular diseases. Serious cardiovascular events, such as myocardial infarction and left ventricular hyperthrophy can be caused by arterial stiffness [2], because the elasticity of the walls of the arteries has a large impact on the blood pressure and the afterload. Increased arterial stiffness (e.g. as a result of coronary heart disease) causes increased systolic blood pressure and pulse pressure, in addition to increased mechanical load on the heart [3].

Ageing is usually associated with degradation of arterial structure and function, such as increased arterial stiffness [4-6]. Recent studies show that decreased arterial elasticity appears early, even before any clinical symptoms or atherosclerotic plaques [7-9].

Therefore, there is an urgent need for early and accurate diagnosis of cardiovascular diseases. In general, existing diagnosis methods relied upon invasive procedures. One such method was Wave Intensity (WI) analysis, introduced by Parker et al.

in 1990 [10]. The wave intensity signal was defined as the product dPxdU, where dP and dU represent the change in pressure and flow, respectively, inside a given blood vessel. However, the clinical use of the WI method was limited because both of the two required parameters (dP and dU) were measured invasively.

Recently, another technique, known as Wave Intensity Wall Analysis (WIWA), was introduced [11]. The idea of WIWA was to estimate the changes in pressure (dP/dt) and flow (dU/dt) by measuring the strain rate of the arterial wall in the radial and longitudinal direction, respectively. While WIWA provides a non-invasive method (using 2D ultrasound image sequences of the carotid artery) for studying blood flow and pressure in the carotid artery based on the principle of conservation of mass and momentum, there are several disadvantages in this approach.

Traditional WI analysis relies upon simultaneously measureing both blood pressure and flow-velocity which is a nontrivial task [12]. Since WI is defined as the product of these two measured quantities, it is very sensitive to noise [12]. Furthermore, the WIWA method estimates these quantities from ultrasound image sequences [11] and suffers from inaccuracy due to the difficulty in estimating longitudinal strain. Therefore, it sounds reasonable to simplify the analysis by limiting it to measuring the radial distension only.

Many methods perform local radial-motion measurements of arterial stiffness by estimating distensibility, compliance, elastic modulus or stiffness index. However, the validity and reproducibility of these measurements show large variation [13-14]. Despite that the main goal of most recent research is to develop methods that can measure deviations from normality, there is still no such method which is free of limitations.Azar and Hamid Muhammed [15] used a self-organizing neural-network to automatically track the motion of the wall of the carotid artery in ultrasound image sequences. However, that approach suffered from the heavy computational load that was required by the self-organizing neural-network. In addition, the goal was to achieve an algorithm for a more efficient and practical WIWA approach, that could automatically produce WIWA signatures of good quality (i.e. can be used to achieve more accurate diagnosis). Therefore, this approach also suffered from the limitations of WIWA technique.

This paper describes time-domain and frequency-domain approaches for automating the diagnosis of the condition of the carotid artery from ultrasound image sequences, by estimating the radial distension only. Since WI analysis is a time domain method, it would be useful to transform the measured time signals into the frequency domain to get a more compact description of the dynamics of these signals.

The main contributions of this work are:

- A time domain method based on radial distension is designed and applied to differentiate among the radial motion of the carotid artery in three categories of cases; healthy young, healthy elderly and pathological elderly patients. The proposed approach is able to demonstrate clear differences in the characteristics of these motion-descriptive curves and can aid medical specialists in diagnosing the physiological condition of the cardiovascular system.
- A frequency domain method is designed to further quantify the differences among these three classes or categories of cases. A spectral feature is utilized as a measure to automatically classify any given case of these classes.
- The proposed approach is simple, non-invasive, reproducible, and presents objective measures (both in time and frequency domains) to aid in achieving accurate diagnosis.

2 Materials and Methods

2.1 Datasets of Ultrasound Image Sequences

Two datasets of ultrasound image sequences were used in this study. The first one was provided by School of Technology and Health, STH, at Royal Institute of Technology, KTH (in collaboration with Karolinska Institute, KI), Stockholm, Sweden. It consisted of nine healthy young cases (31-45 years old) and eight elderly cases (62-70 years old) where two of them were suffering from coronary artery disease. The second data set consisted of totally 34 ultrasound image sequences; 14 healthy elderly cases (56-69 years old) in addition to 20 patients (61-73 years old) suffering from coronary heart disease. This dataset was provided by the Division of Cardiology at Rafik Hariri University Hospital, Beirut, Lebanon.

All experimental studies were approved by the local ethics committees in both Stockholm (Sweden) and Beirut (Lebanon) and all participants gave their informed consent to participate.

2.2Image Segmentation

Extracting vessel walls in an ultrasound image sequence, is a challenging problem mainly due to the low signal-to-noise ratio, unclear boundaries, and varying intensities and shapes across the frames. Therefore, in order to segment these images properly, it is necessary use of both spatial and temporal information in the image sequence. Figure (1) shows a typical image of carotid artery stenosis (CAS), marked by a white ellipse, where the artery gets narrower and its walls become thicker.

At first, the k-means clustering algorithm was implemented to segment each image into three classes (k=3). Three spatial/textural features (mean value, standard deviation, and entropy) were computed in a square neighborhood around each pixel, and used as an input to the k-means algorithm. Figure (2) shows the segmentation result of the frame shown in Figure (1).

In the result presented in Figure (2), it is not easy to recognize vessel wall boundaries from other boundaries. Even a skilled human operator cannot distinguish any characteristic differences by inspecting the result of processing only one stationary image (i.e. one frame of the ultrasonic image sequence). However, the segmentation process gets significantly easier when temporal information is used. Obviously, when the images are set in sequence, motion allows us to differentiate between vessel walls and other tissues, because it is mainly the vessel walls that move while other boundaries are relatively static. For this purpose, the standard deviation, of pixel values across the frames in the image sequence, is utilized to find the vessel walls' pixels which have relatively high standard deviation values.

By this way, the most prominent vessel walls will be selected; i.e. the one that is most dynamic (by choosing the boundaries with high standard deviation) and most visible (when using the k-means algorithm). Figure (3) shows this vessel wall of the image in Figure (1) and its segmentation result in Figure (2).

2.3Automated Region Selection

Initially, in [11] and [15], the user is given the choice of identifying and cropping a region of interest (ROI) in the first frame as shown in Figure (4). One of the problems with this method of manual ROI-selection is that the user may not be able to identify the best location that would give a clear radial distension signal. This problem was encountered by the authors in [11] when using the GE EchoPAC software.

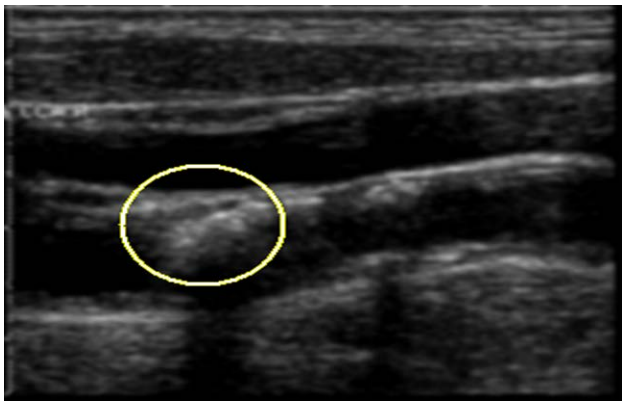

Fig. 1. Carotid artery ultrasound image. The white ellipse marks a stenosis.

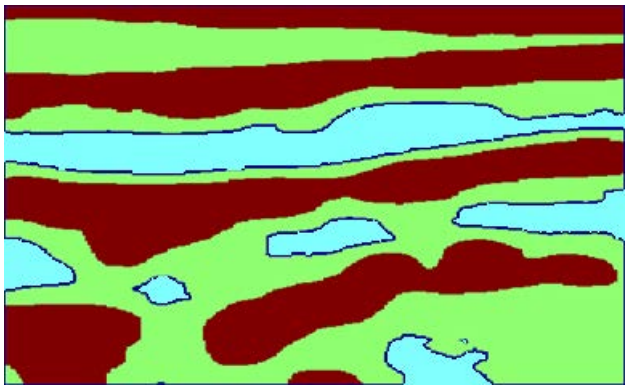

Fig. 2. Segmentation by using k-means, with k=3.

Fig. 3. Extracted vessel wall.

The user would have to often try out several different locations on the vessel wall before obtaining an acceptable radial distension signal from which a WI signal with "classical" apparent characteristics is derived.

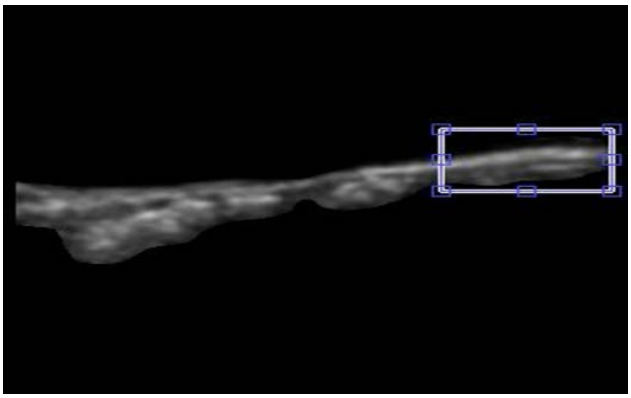

Fig. 4. Manual cropping of a region of interest (ROI) marked by a white rectangle.

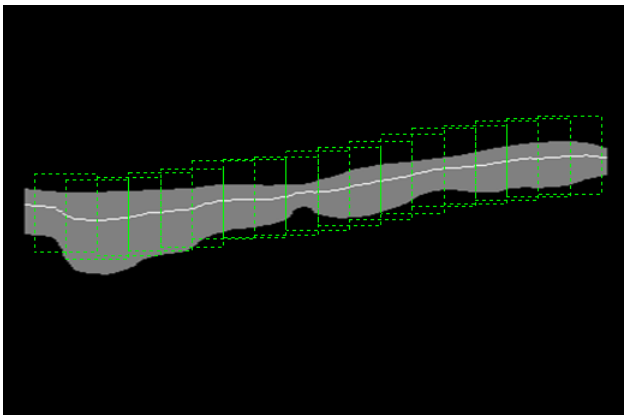

Fig. 5. Regions overlapping midway are assigned along the longitudinal direction of the vessel wall.

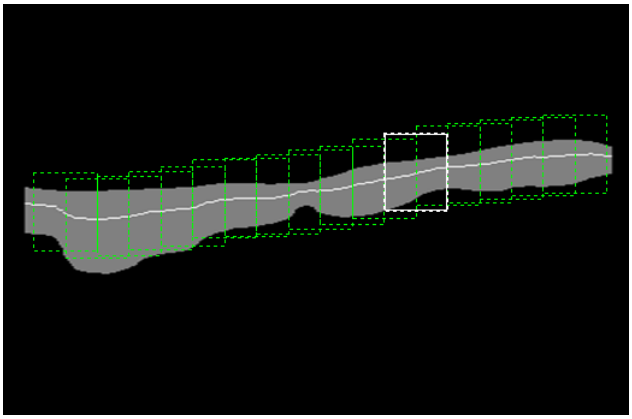

Fig. 6. The region with the largest mean radial variation is automatically selected (marked by a white rectangle).

To circumvent this problem in this paper, region selection was automated based on systematic assignment and evaluation of different overlapping regions along the vessel wall. The method proceeds by, at first, effectively isolating the internal section of the vessel wall that is in contact with the flow of blood. Then, a series of regions are assigned along the longitudinal direction of the vessel wall in a manner such that they overlap midway as shown in Figure (5).

In the evaluation task, the mean radial variation for each region is calculated temporally across the frames. Finally, the region with the largest mean radial variation is selected as marked by a white rectangle in Figure (6). The selected region would be the best candidate from which to obtain a radial distension signal of good quality.

3 Experimental Results

3.1 Time Domain Analysis: Method description, experimental results and discussion

The basic concept is to obtain, from the selected region extracted as described previously, a time dependent signal showing the variation of the lower (inner) vessel boundary in terms of radial position. Figure (7a) illustrates such a signal, aligned with the corresponding Echo-Cardio-Graphy ECG signal in Figure (7b), for the case of a young healthy individual.

The peaks in Figure (7a) are a result of the vessel wall boundary distending upward then downward. For this young healthy case (Y1), it can be easily noticed that the peaks mainly arrive in three consecutive pairs. The motion of the carotid artery was recorded for three heartbeats as indicated by the corresponding ECG signal in Figure (7b); thus each pair of peaks occurs within one ECG cycle (shortly after the QRS complex). It can be noticed that the secondary peak within each pair is almost equal in amplitude to the primary peak. Thus, within each ECG cycle, the vessel wall performs an up-down motion twice in almost an identical fashion. This characteristic pair-of-peaks of the radial distension signal is observed in all nine young healthy cases examined. Figures (8) and (9) illustrate the young healthy cases Y2 and Y3.

We may conclude from these findings that young healthy patients exhibit a clear and almost equal double-peak at the highest level of the radial distension curve. The double peak is an indication that the vessel wall is non-rigid and flexible enough to exhibit an up-down motion twice before completely relaxing to its initial position.

On the other hand, this characteristic pair-of-peaks seems to be absent in all cases of elderly patients who participated in this study. Figure (10) shows the radial distension curve and the corresponding ECG signal for a healthy elderly patient (case E1). Here in Figure (10a) it is possible to notice only one main peak which appears shortly after the QRS complex of the corresponding ECG cycle in Figure (10b). In this case, it is evident that the secondary peak is almost absent in the radial distension curve. A possible explanation is that the vessel wall is stiff and unable to return upwards a second time before descending back to its initial position.

Another elderly case, but this time a pathological one, suffering from coronary artery disease (EP1), is shown in Figure (11). From the result of this case and all other pathological elderly patients (suffering from coronary artery disease) who were examined, we may conclude that in such cases the secondary peak is always either absent or, in best case, significantly weaker in amplitude than the primary peak. In addition, more irregular radial distension profiles were obtained in the cases of pathological elderly patients when compared to healthy elderly cases.

These characteristic differences in the radial distension curve (among the three categories of cases considered in this study) can aid medical specialists in easily identifying problems in the carotid artery and obtaining an idea on the stiffness of the artery. Certainly, such curves are much easier to interpret and can help in giving a clearer insight into the motion of the vessel wall than what can be obtained from only observing an ultrasound image sequence of the carotid artery. In addition, these radial distension curves are extracted from the ultrasound image sequences in an automated manner as illustrated in the previous sections.

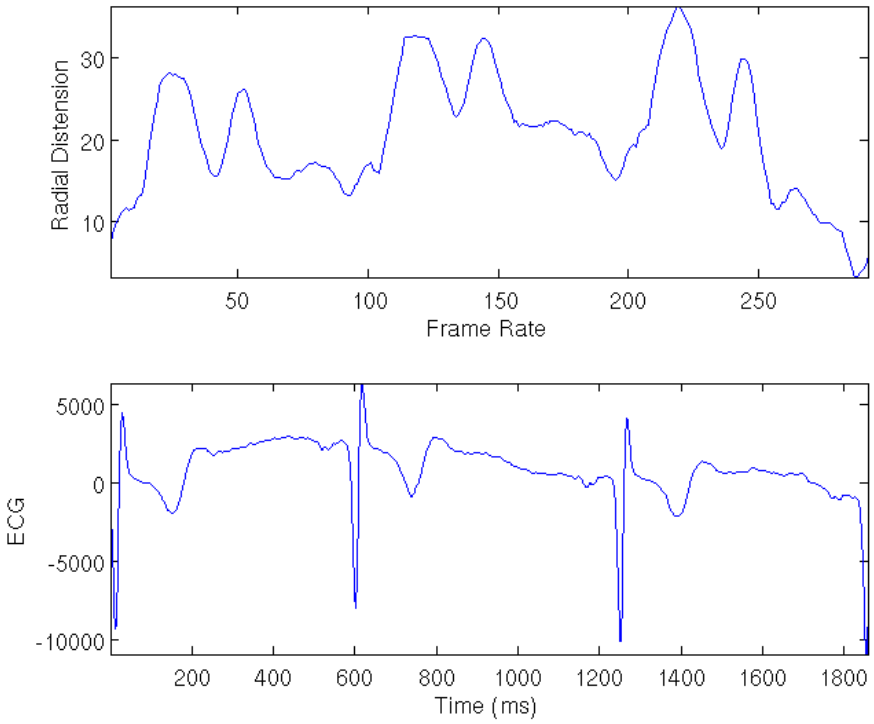

Fig 7. (a) Radial distension profile for the young healthy case Y1. (b) The corresponding ECG signal.

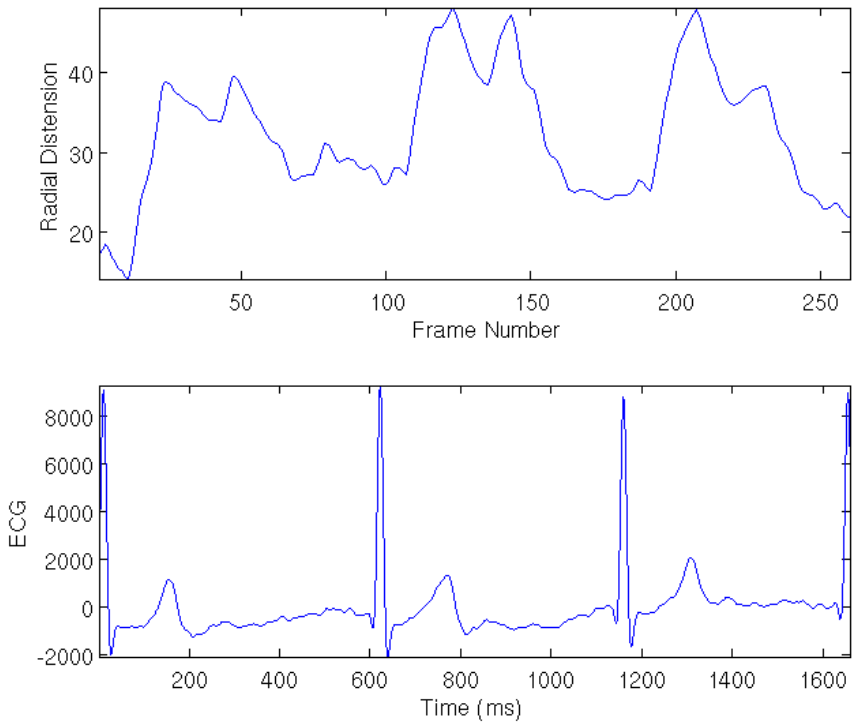

Fig. 8. (a) Radial distension profile for the young healthy case Y2. (b) The corresponding ECG signal.

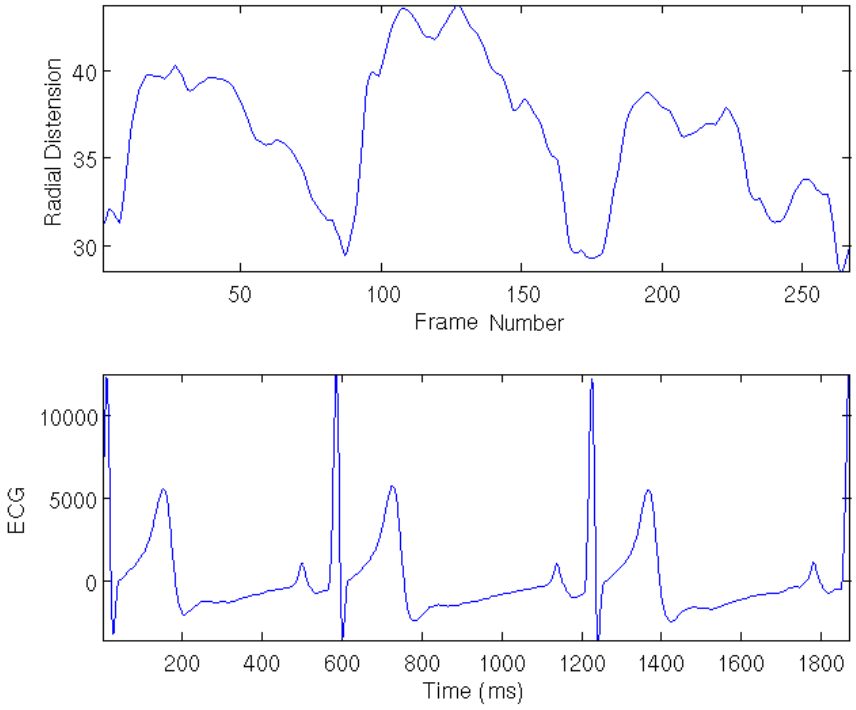

Fig 9. (a) Radial distension profile for the young healthy case Y3. (b) The corresponding ECG signal.

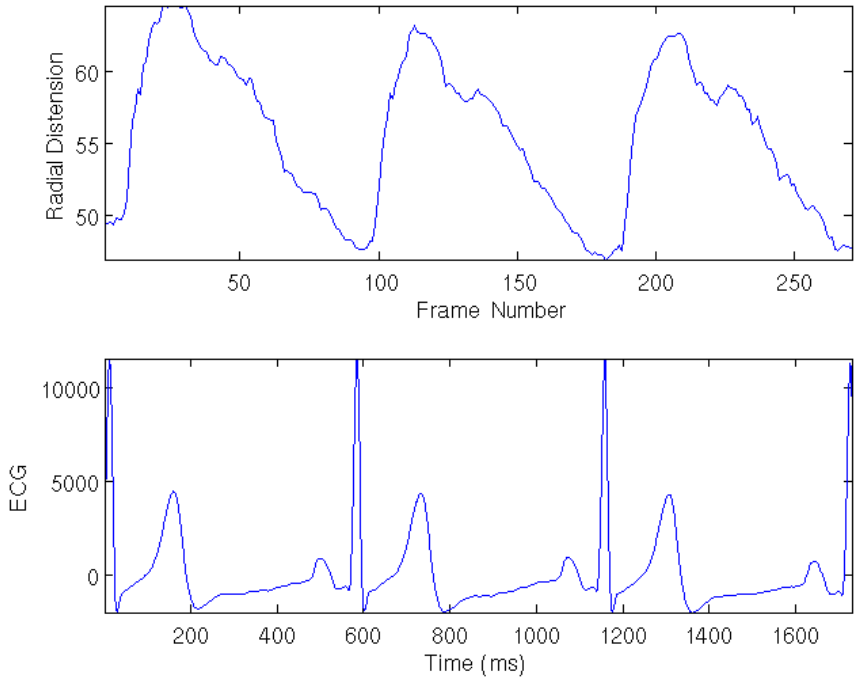

Fig. 10. (a) Radial distension profile for the elderly case E1. (b) The corresponding ECG signal.

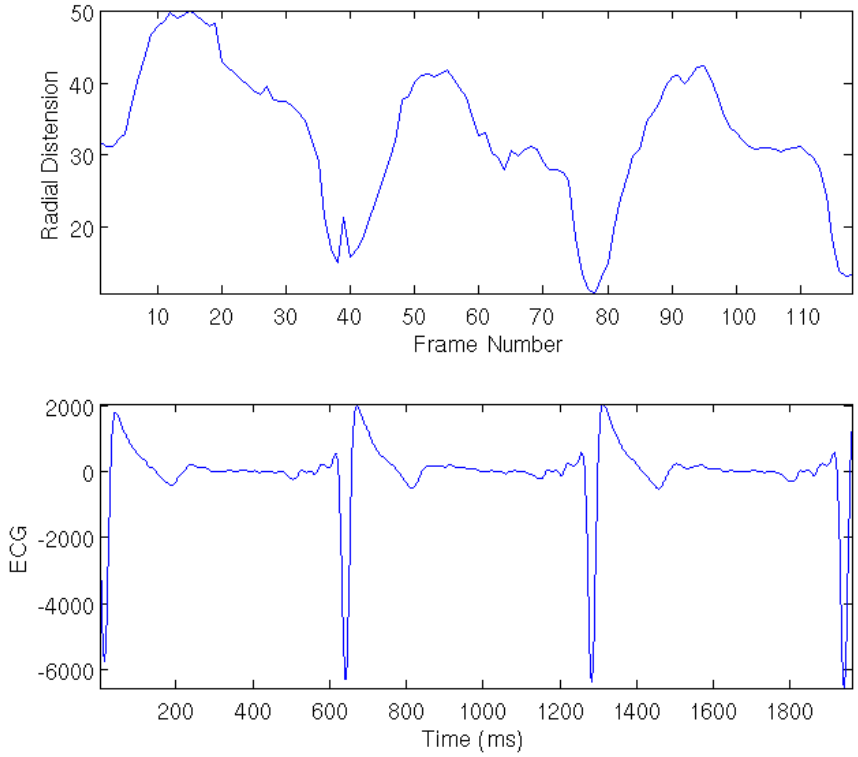

Fig. 11. (a) Radial distension profile for thepathological elderly case EP1. (b) The corresponding ECG signal.

3.2 Frequency Domain Analysis: Method description, experimental results and discussion

The time domain approach discussed so far is completely automated, however the end result is a radial distension curve, that can be analyzed by a medical expert, in addition to visually inspecting the ultrasound image sequence. To help further quantify and automate the decision process, a useful feature has to be derived from the radial distension signals. As a first task for this purpose, the time domain signal is transformed into the frequency domain via the Discrete Fourier Transform (DFT). Figure (12) shows the DFT results of one healthy young case (Y1) and one healthy elderly case (E1).

Note that the first element of each DFT result, which is the DC value, is discarded from all calculations, since it is scale dependent. The area subtended by the transform is then calculated (i.e. for the range of normalized frequencies $0 < f \leq 1$) and utilized as a diagnostic feature to differentiate among different cases.

Furthermore, in the last step, all frequency elements above a normalized frequency of 0.15 are also discarded and the corresponding areas are calculated, for normalized frequencies greater than 0 and up to 0.15 ($0 < f \leq 0.15$). The new spectral-area measure (which is less biased by useless high frequency components with respect to our purpose) is also utilized as a diagnostic feature. The latter measure can be used to achieve a more efficient differentiation among the three classes of cases considered in this study.

Both of these two variants of the frequency domain analysis method are tested against all cases of the two datasets. The resulting spectral-area values (for normalized frequencies $0< f \leq 1$ and $0 < f \leq 0.15$) are presented in Figure (13). It can be easily observed that both of the two spectral-area features are dominantly higher in value in healthy young cases than in healthy as well as pathological elderly patients. Furthermore, both features are higher in healthy elderly cases than pathological elderly patients.

For normalized frequencies $0 < f \leq 1$, all elderly cases had feature values below 12.1, whereas all young cases had values above 18.4. Therefore, a threshold value of 15.25 may be used to differentiate between young and elderly cases. While for normalized frequencies $0 < f \leq 0.15$, a threshold value of 10.3 can be used to perform this differentiation, because all elderly cases had feature values below 8, while all young cases had values above 12.6.

It can be easily noticed that the derived feature values (i.e. the spectral area measures) for the young group are better separated from those derived for the elderly group, when only considering the normalized frequencies $0 < f \leq 0.15$.

When considering only the elderly groups, threshold values of 6.75 and 4.4 can be used to differentiate between healthy and pathological patients for the two features derived for the normalized frequencies$0 < f \leq 1$ and $0 < f \leq 0.15$, respectively.

Here also, better separation is obtained between the feature values of these two groups of elderly patients, when using the normalized frequencies $0 < f \leq 0.15$. The feature values for all pathological cases are below 6.3 and 3.6 when considering the normalized frequencies$0 < f \leq 1$ and $0 < f \leq 0.15$, respectively. While, the corresponding values are above 7.2 and 5.2, respectively, for the healthy cases.

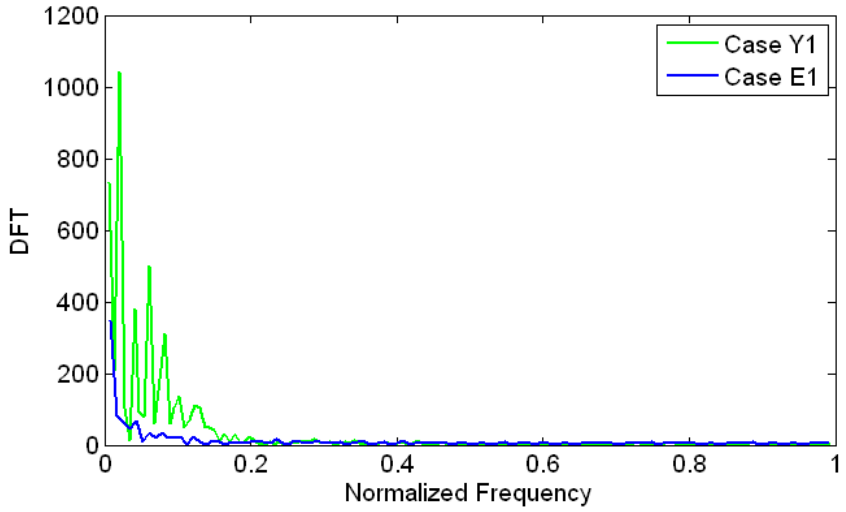

Fig. 12. Discrete Fourier transform results, for the young case Y1 (green curve) and for the elderly case E1 (blue curve).

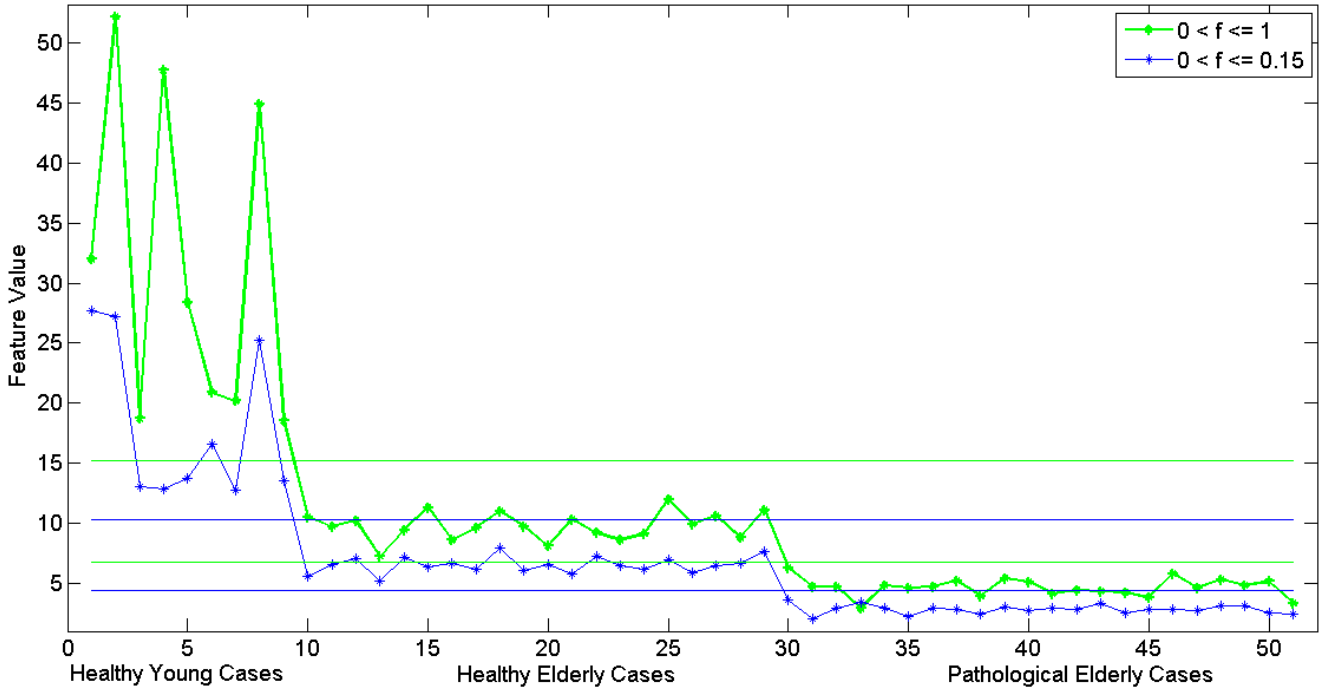

Fig. 13. Feature values (spectral area values) forhealthy young cases,healthy elderly cases and pathological elderly cases, for normalized frequencies $0 < f \leq 1$ (green curve)and $0< f \leq 0.15$ (blue curve). The thresholds that were selected and used to differentiate among these three categories or classes when considering each of the two cases of normalized frequencies are shown as two green horizontal lines for $0< f \leq 1$ and as two blue horizontal lines for $0 < f \leq 0.15$.

4 Conclusion

In this study, a novel approach for automating the classification of the physiological condition of the carotid artery in 2D ultrasound image sequences was presented. The new approach utilizes the radial distension properties of the inner vessel wall of the carotid artery to obtain insight about the stiffness of the artery and its relaxation capacity with time. This can aid medical specialists in assessing the condition of the carotid artery.

To facilitate further such an assessment, two relevant features were derived from the discrete Fourier transform of the radial distension signal and these were utilized to automatically differentiate among healthy young, healthy elderly and pathological elderly cases. Suitable threshold values were identified and used for classification. A thresholding classifier, which used two threshold values, was utilized for each of the two derived features discussed previously to differentiate among the three classes or categories in this study.

With enough data samples (i.e. ultrasonic videos) as input, a more advanced classifier such as a support vector machine may be constructed to automatically differentiate between for example two classes of healthy and pathological patients based on deriving and using these two spectral-area features.

This computer-aided method would significantly simplify the task of medical specialists in detecting any defects in the condition of the carotid artery and thereby in detecting cardiovascular symptoms. This opens up the possibility for the use of machine learning in the automatic classification of different arterial characteristics among different categories of patients.

The elegance and efficiency of the proposed non-invasive time-domain and frequency-domain methods stem from a number of desired properties that these methods enjoy, such as that they are intuitive, straightforward, simple, semi-automatic (supervised since the threshold values were identified and chosen by the user or the operator of this system), reproducible, and reduces the reliance upon subjective measures significantly.

Acknowledgements

The authors would like to thank Prof. Dr. Lars-

ÅkeBrodin, Dr. Matilda Larsson and Dr. Anna Bjällmark (at School of Technology and Health, Royal Institute of Technology, Stockholm, Sweden) for fruitful discussion as well as providing and sharing their datasets of ultrasound image sequences and knowledge and experience about WIWA.

The authors are also grateful to Dr. George Rustom at Rafik Hariri University Hospital, Beirut, Lebanon, for providing and sharing their useful datasets of ultrasound image sequences.

References

[1] E. Gebel, "Heart Disease a Leading Cause of Death Worldwide," State Department's Bureau of International Information Programs (IIP), USA, 2008.

[2] S. Stork, A.W. van den Beld, C. von Schacky, C.E. Angermann, S.W.J. Lamberts, D.E. GrobbeeE, M.L. Bots, "Carotid Artery Plaque Burden, Stiffness, and Mortality Risk in Elderly Men. A Prospective, Population-Based Cohort Study," *Circulation*, vol. 110, no. 3, pp. 344-348, 2004.

[3] C. Chae, M. Pfeffer, R. Glynn, G. Mitchell, J. Taylor, C. Hennekens, "Increased pulse pressure and risk of heart failure in the elderly," *JAMA*, vol. 281, pp. 634-639, 1999.

[4] A. Benetos, B. Waeber, J. Izzo, G. Mitchell, L. Resnick, R. Asmar, M. Safar, "Influence of age, risk factors, and cardiovascular and renal disease on arterial stiffness: clinical applications," *Am. J. Hypertens.*, vol. 15, no. 12, pp. 1101-1108, 2002.

[5] C.M. McEniery, Yasmin, I.R. Hall, A. Qasem, I.B.Wilkinson, J.R. Cockcroft, "Normal Vascular Aging: Differential Effects on Wave Reflection and Aortic Pulse Wave Velocity - The Anglo-Cardiff Collaborative Trial (ACCT)," *J. Am. Coll. Cardiol.*, vol. 46, pp. 1753-1760, 2005.

[6] G.F. Mitchell, H. Parise, E.J. Benjamin, M.G. Larson, M.J. Keyes, J.A. Vita, R.S. Vasan, D. Levy, "Changes in Arterial Stiffness and Wave Reflection with Advancing Age in Healthy Men and Women: The Framingham Heart Study," *J. Hypertens.*, vol. 43, no. 6, pp. 1239-1245, 2004.

[7] S. Glasser, D. Arnett, G. McVeigh, S.M. Finkelstein, A.J. Bank, D.J. Morgan, J.N. Cohn, "Vascular compliance and cardiovascular disease: a risk factor or a marker?," *Am. J. Hypertens.*, vol. 10, no. 10, pp. 1175-1189, 1997.

[8] S. Laurent, P. Boutouyrie, "Arterial stiffness: a new surrogate end point for cardiovascular disease?," *J. Nephrol.*, vol. 20, pp. 45-50, 2007.

[9] F.U.S. Mattace-Raso, T.J.M. van der Cammen, A. Hofman, N.M. van Popele, M.L. Bos, M.A.D.H. Schalekamp, R. Asmar, R.S. Reneman, A.P.G. Hoeks, M. Breteler, J.C.M. Witteman, "Arterial Stiffness and Risk of Coronary Heart Disease and Stroke," *The Rotterdam Study*, *Circulation*, vol. 113, no. 5, pp. 657-663, 2006.

[10] K. Parker, C.J.H. Jones, "Forward and Backward Running Waves in the Arteries: Analysis Using the Method of Characteristics," *J. Biomech. Eng.*, vol. 112, no. 3, pp. 322-326, 1990.

[11] M. Larsson, A. Bjällmark, B. Lind, R. Balzano, M. Peolsson, R. Winter, L-A Brodin, "Wave Intensity Wall Analysis: a novel non-invasive method to measure wave intensity," *Heart and Vessels*, vol. 24, no. 5, pp. 357-365, 2009.

[12] K. Parker, "An Introduction to Wave Intensity Analysis," *Med. Biol. Eng. Comput.*, vol. 47, pp. 175-188, 2009.

[13] P.K. Hamilton, C.J. Lockhart, C.E. Quinn, G.E. McVeigh, "Arterial stiffness: clinical relevance, measurement and treatment," *Clinical Science*, vol. 113, pp. 157-170, 2007.

[14] B.M. Pannier, A. Avolio, A. Hoeks, G. Mancia, K. Takazawa, "Methods and devices for measuring arterial compliance in humans," *Am. J. Hypertens.*, vol. 15, pp. 743-753, 2002.

[15] J.C. Azar, H. Hamid Muhammed, "Automated Tracking of the Carotid Artery in Ultrasound Image Sequences Using a Self Organizing Neural Network," in *Proc. 20th Intl Conf. Pattern Recognition ICPR 2010*, Istanbul, Turkey, 2010.